Control Theory and Technology (2023) 21:97–109
https://doi.org/10.1007/s11768-023-00131-4

RESEARCH ARTICLE

On the notions of normality, locality, and operational stability in ADRC

Huiyu Jin[1] · **Zhiqiang Gao**[2]

Received: 1 November 2022 / Revised: 20 January 2023 / Accepted: 26 January 2023 / Published online: 14 March 2023

Abstract
Treating plant dynamics as an ideal integrator chain disturbed by the total disturbance is the hallmark of active disturbance rejection control (ADRC). To interpret its effectiveness and success, to explain why so many vastly different dynamic systems can be treated in this manner, and to answer why a detailed, accurate, and global mathematical model is unnecessary, is the target of this paper. Driven by a motivating example, the notions of normality and locality are introduced. Normality shows that, in ADRC, the plant is normalized to an integrator chain, which is called local nominal model and locally describes the plant's frequency response in the neighborhood of the expected gain crossover frequency. Locality interprets why ADRC can design the controller only with the local information of the plant. With normality and locality, ADRC can be effective and robust, and obtain operational stability discussed by T. S. Tsien. Then viewing proportional-integral-derivative (PID) control as a low-frequency approximation of second-order linear ADRC, the above results are extended to PID control. A controller design framework is proposed to obtain the controller in three steps: (1) choose an integrator chain as the local nominal model of the plant; (2) select a controller family corresponding to the local nominal model; and (3) tune the controller to guarantee the gain crossover frequency specification. The second-order linear ADRC and the PID control are two special cases of the framework.

Keywords Active disturbance rejection control · Normality · Locality · Local nominal model · Bode plot · Operational stability · Design framework

1 Introduction

Active disturbance rejection control (ADRC), conceived by Han [1–3] as a general purpose control technology and an alternative to the industry-dominant proportional-integral-derivative (PID) control, has developed rapidly in recent years, in both engineering practice (see, for example, [4–6]) and theoretical studies (see, for example, [7,8]).

The idea of ADRC can be traced to T. S. Tsien. In Chap. 15 of his epic book titled "Engineering Cybernetics" [9], Tsien flatly said that the mathematical model of a physical plant can never be known exactly in practice and should not be the basis on which to design the controller. Furthermore, with the example of airplane under icing conditions, Tsien emphasizes that the control system design must face large, unpredictable variations of the plant and maintain its operational stability. Unfortunately, his advice has been largely ignored in academic studies, where rigor was attained at the expense of shifting the object of study. The object shifted from the real physical processes, with all their uncertainties and imperfections, to a set of mathematical equations that are assumed to accurately described the dynamics of the plant to be controlled. The result has been the ever-widening divide between theory and practice witnessed by all. The later developments, such as those in the area of adaptive control [10], attempt to mediate the discrepancies between the model and the actual dynamics but offer few tangible improvements.

In China, however, Tsien's penetrating insight was not entirely lost. In a survey paper titled "Certain issues in mod-

Huiyu Jin and Zhiqiang Gao contributed equally to this work.

This work was supported by the National Nature Science Foundation of China (Grant No. 61733017).

✉ Huiyu Jin
jinhy@xmu.edu.cn

Zhiqiang Gao
z.gao@ieee.org

[1] School of Aerospace Engineering, Xiamen University, Xiamen 361102, Fujian, China

[2] Center for Advanced Control Technologies, Cleveland State University, Cleveland, OH 44115, USA

ern control theory" and published in 1980 [11], Guan points out the issue of model dependency in modern control theory and the problem of disturbance it mostly ignored. He asserts that the frequency response method favored by engineers is based on the fundamental principle that the closed-loop system behavior largely depends on open-loop characteristics near the crossover frequency. He further suggests that such deep engineering insight must be somehow combined with the theoretical studies of optimality and stability. In essence, what Guan implies that, for the purpose of feedback design, open loop dynamics needs to be known only locally, in the neighborhood of the gain crossover frequency.

Tsien returned to China shortly after the publication of [9] and never returned to the field of control theory. It was Han who answered Tsien call in 1989 [12] and flatly called the modern control theory a theory about model, not necessarily control. He insists that a physical process should be controlled based on its characteristics local in time and space, not some mathematical model assumed to be detailed and accurate the entire time, through all phases of operations. It would take him the next twenty years to conceive and develop an epic solution to this challenge, in the form of ADRC.

Key to ADRC, above all, is the proposition that the physical plants are to be treated as an ideal integrator chain disturbed by total disturbance. The total disturbance includes external disturbance and internal disturbance, which is Tsien's notion and can be understood here as the lumped result of the dynamics and uncertainties internal to the plant and make the plant different from the integrator chain. In other words, in ADRC, model is redefined as one that describes the ideal dynamics of the integrator chain, instead of actual dynamics of a particular physical process.

With an integrator chain and total disturbance, ADRC provides a framework to solve the control problem. It establishes an extended state observer (ESO) to estimate the total disturbance in real time. Then, the estimation is canceled and the plant is controlled as an integrator chain. With continuously estimating and canceling, ADRC forces the plant to behave like the ideal integrator chain, while the controller design becomes straightforward.

Even though ADRC has found successful applications in many fields of engineering practice, its universality has yet to be established theoretically. To this end, it is shown in [13] that any linear finite-dimensional controller can be implemented via the linear ADRC (LADRC) structure, but this still left one wondering what makes such structure so prevalence. What is hidden in ADRC that captured the hidden commonalities among different fields of control engineering? This question provides the main motivation for this paper.

To explain the mechanism of ADRC, this paper introduces the notions of normality and locality. Normality refers to the property of the design methods to normalize those physical plants as an integrator chain. While locality, as discussed by Han and Guan, means for the purpose of control design, the design methods such as ADRC and PID control can obtain controller mainly with the plant's local information. That is, the dynamics of the physical plants only need to be described as an integrator chain near the expected gain crossover frequency. Furthermore, it illustrates with examples that operational stability discussed by Tsien is a result of normality and locality.

The rest of this paper is organized as follows. Section 2 revisits a motivating example and introduces the second-order LADRC. The example is proposed by [14] and sparks persistent interest in frequency response and robustness research of ADRC [15–21]. Section 3 proposes the concept of local nominal model and discusses the notions of locality, normality, and operational stability. Section 4 illustrates the locally shaping ability of the second-order LADRC and the PID control. Section 5 establish the locality of the second-order LADRC and the PID control, and proposes a new design framework. The paper ends with a few concluding remarks in Sect. 6.

2 The motivating example

In this section, we briefly revisit the example in [14,16], which is typically used in robust control research of ADRC. Using it as an motivating example, we introduce the second-order LADRC and illustrate how it guarantees stability and robustness for the plant with parametric uncertainty.

2.1 The plant

Consider the plant

$$\begin{cases} \dot{x}_1 = x_2, \\ \dot{x}_2 = -a_2 x_1 - a_1 x_2 + b(u + w), \end{cases} \tag{1}$$

$$y = x_1, \tag{2}$$

where x_1, x_2 are the state, u, y, and w are, respectively, the input, output, and external disturbance. The parameter $b = 206.25$, while $a_1, a_2 \geq 0$ but uncertain.

Obviously, the plant (1)–(2) has transfer function

$$P(s) = \frac{Y(s)}{U(s) + W(s)} = \frac{b}{s^2 + a_1 s + a_2}. \tag{3}$$

2.2 Second-order LADRC and its transfer function

Now we introduce the second-order LADRC and control (1)–(2) with it. The second-order ADRC views the plant as

$$\ddot{y} = b_0 u + f, \tag{4}$$

where b_0 is a tuning parameter, while f is called as total disturbance. For (1)–(2), we have

$$f = -a_2x_1 - a_1x_2 + (b - b_0)u + bw.$$

Introducing extended state $x_3 = f$, equation (4) is written as

$$\begin{cases} \dot{x}_1 = x_2, \\ \dot{x}_2 = x_3 + b_0u, \\ \dot{x}_3 = \dot{f}, \\ y = x_1. \end{cases}$$

Then a linear ESO (LESO) is established as

$$\begin{cases} \dot{\hat{x}}_1 = \beta_1(y - \hat{x}_1) + \hat{x}_2, \\ \dot{\hat{x}}_2 = \beta_2(y - \hat{x}_1) + \hat{x}_3 + b_0u, \\ \dot{\hat{x}}_3 = \beta_3(y - \hat{x}_1), \end{cases} \tag{5}$$

where $\beta_1, \beta_2, \beta_3$ are tuning parameters. And the controller is

$$u = \frac{1}{b_0}[l_2(r - \hat{x}_1) - l_1\hat{x}_2 - \hat{x}_3], \tag{6}$$

where l_1, l_2 are the tuning parameters. LESO (5) and controller (6) are the second-order LADRC.

LADRC (5)–(6) has six tuning parameters. To simplify, reference [14,16]suggest to generate the parameters $\beta_1, \beta_2, \beta_3$ and l_1, l_2 with

$$\beta_1 = 3\omega_o, \quad \beta_2 = 3\omega_o^2, \quad \beta_3 = \omega_o^3, \tag{7}$$

$$l_1 = 2\omega_o, \quad l_2 = \omega_o^2, \tag{8}$$

where ω_o is a parameter called as ESO bandwidth. Thus, the LADRC has only two parameters ω_o and b_0.

Substituting (6) into (5) and with (7)–(8), we have

$$\begin{cases} \dot{\hat{x}}_1 = -3\omega_o\hat{x}_1 + \hat{x}_2 + 3\omega_o y, \\ \dot{\hat{x}}_2 = -4\omega_o^2\hat{x}_1 - 2\omega_o\hat{x}_2 + 3\omega_o^2 y + \omega_o^2 r, \\ \dot{\hat{x}}_3 = -\omega_o^3\hat{x}_1 + \omega_o^3 y, \end{cases} \tag{9}$$

Viewing y and r as two inputs of (9), while u in (6) as the output, we have the transfer functions

$$\frac{U(S)}{Y(s)} = -\frac{\omega_o^3(10s^2 + 5\omega_o s + \omega_o^2)}{b_0 s(s^2 + 5\omega_o s + 10\omega_o^2)},$$

$$\frac{U(S)}{R(s)} = \frac{\omega_o^2(s + \omega_o)^3}{b_0 s(s^2 + 5\omega_o s + 10\omega_o^2)},$$

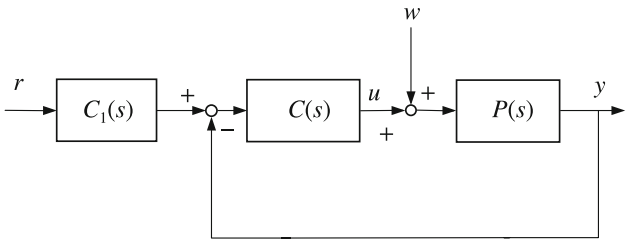

Fig. 1 Block diagram of the second-order LADRC system

where $U(s)$, $Y(s)$, and $R(s)$ are respectively the Laplace transform of u, y, and r. Let

$$C(s) = \frac{\omega_o^3(10s^2 + 5\omega_o s + \omega_o^2)}{b_0 s(s^2 + 5\omega_o s + 10\omega_o^2)}, \tag{10}$$

$$C_1(s) = \frac{(s + \omega_o)^3}{\omega_o(10s^2 + 5\omega_o s + \omega_o^2)}, \tag{11}$$

the second-order LADRC has equation

$$U(s) = C(s)[C_1(s)R(s) - Y(s)]. \tag{12}$$

Equation (12) describes how to generate u with r and y, while (3) describes how the plant generates y with u and w. With them, the second-order LADRC system has a block diagram shown in Fig. 1.

Remark 1 Note here we say the second-order LADRC "views" the plant as (4). It emphasizes in (4), the order two and the parameter b_0 are selected by the engineer. For the second-order LADRC, the plant (1)–(2) is a special case whose order and relative degree are both two. Such a plant is suitable to introduce the second-order LADRC because the total disturbance can be clearly described, while it is well known that the second-order LADRC can be used for the more complicated plants.

Remark 2 Fig. 1 illustrates an advantage of viewing the plant as (4). Suppose we have a plant whose transfer function is $P(s)$. By viewing it as (4), we obtain LADRC (5)–(6) and Fig. 1. Note in the procedure we do not use the plant's information such as order, relative degree, and time-delay. That is, no matter what the plant's order, relative degree, and time-delay are, it can be controlled by the second-order LADRC, while the stability and performance of the closed-loop system can be analyzed with Fig. 1.

2.3 Stability and robustness

With Fig. 1, the stability and robustness of the LADRC system depends on the closed-loop made of $C(s)$ and $P(s)$.

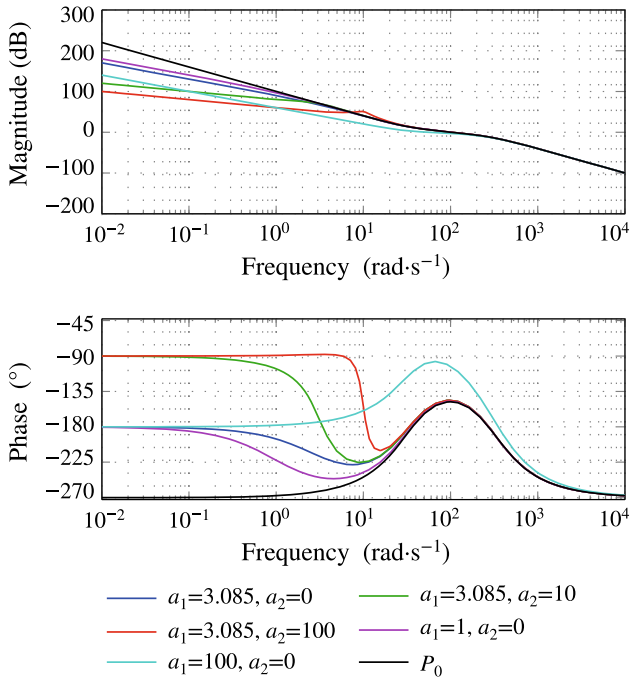

Fig. 2 Bode plots of $P(s)C(s)$ and $P_0(s)C(s)$

In LADRC (5)–(8), let $b_0 = 206.25$, $\omega_o = 100$. For the following five typical pairs:

$$(a_1, a_2) \in \{(3.085, 0), (3.085, 10), (3.085, 100), (1, 0), (100, 0)\}, \tag{13}$$

the Bode plots of $P(s)C(s)$ are drawn in Fig. 2. Let

$$P_0(s) = \frac{b}{s^2}.$$

the Bode plot of $P_0(s)C(s)$ is also drawn. Obviously, all the five pairs are stable. When

$$(a_1, a_2) \in \{(3.085, 0), (3.085, 10), (3.085, 100), (1, 0)\}, \tag{14}$$

the gain crossover frequency is near 100 rad/s, the phase margins is near 31.9°. For the pair $(a_1, a_2) = (100, 0)$, the gain crossover frequency is 53.2 rad/s, while phase margin is 81.2°.

Figure 2 shows the second-order LADRC is robust subject to the plant's significant variation. Such robustness is also reported by [15], where the plant may be unstable. In the rest of this paper, we interpret the robustness with the frequency response method.

3 Normality, locality, and operational stability

In this section, we introduce the concept of the local nominal model and show integrator chain can be widely used as a local nominal model. Then we discuss normality, locality, and operational stability of LADRC.

3.1 Local nominal model

Definition 1 (Local nominal model) Suppose we have a plant $P(s)$ while $P_0(s)$ is another transfer function. $P_0(s)$ is said a local nominal model of $P(s)$ at frequency $\omega_\gamma \geq 0$, if when $\omega \approx \omega_\gamma$, we have $P(j\omega) \approx P_0(j\omega)$.

The purpose of a local nominal model is to describe the plant at ω_γ with a simple model, where ω_γ is usually the expected gain crossover frequency of the loop transfer function to design. Thus, because of its simplicity, the integrator chain

$$P_0(s) = \frac{b}{s^n} \tag{15}$$

is a suitable candidate for a local nominal model. In this paper, we only use (15) as local nominal model.

When (15) is a local nominal model at ω_γ, the plant's frequency response is similar to (15) in the band near ω_γ. Or, intuitively, the plant can be viewed as a distorted integrator chain but the distortion is ignorable near ω_γ. Thus, a simple approach to check if (15) is a local nominal model is to draw the plant's Bode diagram. Note (15) has

$$|P_0(j\omega)| = \frac{b}{\omega^n},$$
$$\angle P_0(j\omega) = -n \cdot 90°.$$

If near ω_γ, the slope of the magnitude-frequency plot approximates $-n$ while the phase approximates $-n \cdot 90°$, then (15) is a local nominal model at ω_γ.

In ADRC, local nominal model (15) corresponds to Han canonical form

$$\frac{\mathrm{d}^n}{\mathrm{d}t^n} y = b_0 u + f, \tag{16}$$

where f is total disturbance. That is, when the plant is written as (16), the local nominal model (15) is implicitly used.

The following are two special cases of $n = 2$, where integrator chain (15) becomes double integrator

$$P_0(s) = \frac{b}{s^2}. \tag{17}$$

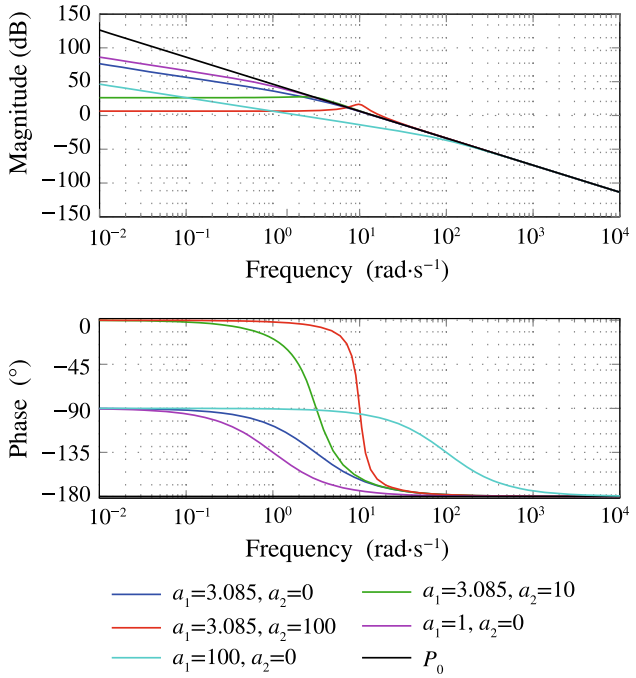

Fig. 3 Bode plots of $P(s)$ and $P_0(s)$ in Example 1

In this paper, we mainly focus on and illustrate the special case of $n = 2$, while the results can be generalized to the integrator chains with other orders.

Example 1 Consider the plant in Sect. 2.1. With (3), it has frequency response

$$P(\mathrm{j}\omega) = \frac{b}{(\mathrm{j}\omega)^2 + a_1(\mathrm{j}\omega) + a_2}.$$

When $\omega \to +\infty$, the term $(\mathrm{j}\omega)^2$ is dominant in the denominator so that

$$P(\mathrm{j}\omega) \approx \frac{b}{(\mathrm{j}\omega)^2} = P_0(\mathrm{j}\omega).$$

Thus, when ω is large enough, the frequency response of (3) approximates that of double integrator (17). For the five pairs in (13), the Bode plots of (3) are drawn in Fig. 3. With (17) and $b = 206.25$, Bode plot of $P_0(s)$ is also drawn with black line. Obviously, all six plots are close in high-frequency. At frequency $\omega_\gamma = 100$, the plants with the four pairs in (14) have (17) as a local nominal model. Even for the pair $(a_1, a_2) = (100, 0)$, double integrator (17) can be viewed as a local nominal model.

Example 2 Consider the plant

$$P_1(s) = \frac{1}{(s+1)^3}, \tag{18}$$

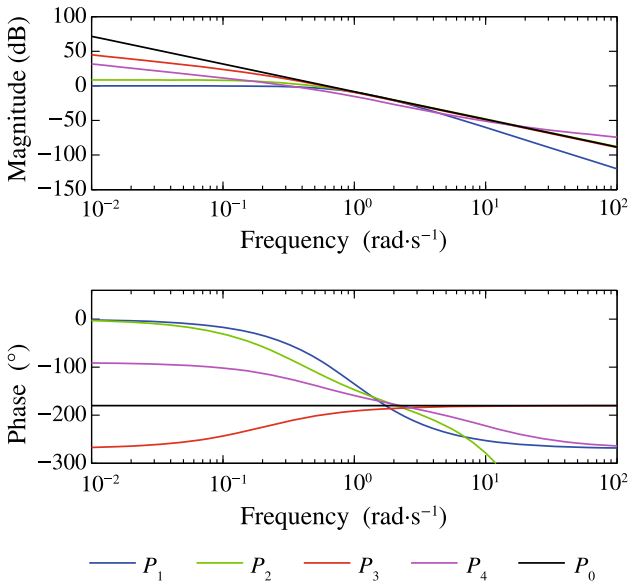

Fig. 4 Bode plots of $P(s)$ and $P_0(s)$ in Example 2

$$P_2(s) = \frac{0.40}{(s+0.1)(s+0.3)}\mathrm{e}^{-0.18s}, \tag{19}$$

$$P_3(s) = \frac{0.36}{s(s-0.2)}, \tag{20}$$

$$P_4(s) = \frac{0.0191(20-s)}{s(s+0.5)}, \tag{21}$$

and let

$$P_0(s) = \frac{0.38}{s^2}. \tag{22}$$

The Bode plots of (18)–(22) are shown in Fig. 4. It is shown that the plant (22) is a local nominal model of plant (18)–(21) respectively at $\omega_1 = 1.7$, $\omega_2 = 2.0$, $\omega_2 = 6.0$, and $\omega_4 = 3.0$. It means if we control $P_1(s)$, $P_2(s)$, $P_3(s)$, and $P_4(s)$ and specify their loop transfer functions' gain crossover frequency respectively at $\omega_1 = 1.7$, $\omega_2 = 2.0$, $\omega_2 = 6.0$, and $\omega_4 = 3.0$, we can use (22) as their local nominal model.

Remark 3 Definition 1 uses "$\approx$" instead of inequality constraint. The reasons are the following two. First, for engineering practice, "$\approx$" is clear enough and used in classic textbooks such as [22]; second, we have not found a suitable strict inequality constraint. Empirically and with Bode plot, we suggest that at ω_γ, if the slope of the magnitude-frequency plot is in $(-n-0.5, -n+0.5)$ and the phase is in $(-n \cdot 90° - 15°, -n \cdot 90° + 45°]$, then (15) can be used as a local nominal model.

Remark 4 When (15) is a local nominal model, its parameter b is not unique. For example, in Example 1, if we let $b = 200$,

the plants with pairs of (13) all have the local nominal model (17) at frequency $\omega_\gamma = 100$.

Remark 5 Example 1 can be generalized to that for all stable minimum-phase plants with relative degree n, integrator chain (15) is a local nominal model at a large enough frequency. This property is why ADRC usually chooses the plant's relative degree as its order.

Remark 6 Note (18)–(21) are four typical plants. The plant (18) is a stable and minimal-phase plant whose order and relative degree are not two. The plant (19) has time-delay. The plant (20) has an unstable zero, while (21) is unstable. Example 2 shows that the local nominal model provides a unified approach to deal with them.

3.2 Normality

Now we discuss normality. Suppose we have a method to design controller. We say the method has normality if it first normalizes the plant to a local nominal model. For example, with Example 1 and Sect. 2, we conclude the second-order LADRC has normality because it normalizes the plant to double integrator (17) first. PID control also has normality and we illustrate it later.

Normality partly explains why so many vastly different plants in various fields of engineering can be treated as Han canonical form (4). The reason is, these plants can have local nominal model (17) at the expected gain crossover frequency. Thus, the second-order LADRC normalize them to (17) and control them.

Normality has two advantages. First, it simplifies the controller design to obtain a controller for integrator chain (15), which is relatively easy to control. Second, it guarantees the robustness of the method. It means several plants, maybe quite different, can share a common local nominal model and a common controller. That is, the method can obtain a controller with perfect robustness.

3.3 Locality

Locality is also a property of the design method. We say the method has locality if it is mainly based on local information to design and can guarantee stability when used for the plant. Both the second-order LADRC and the PID control have locality. They design the controller with the local nominal model (17), which contains the local information of the plant around the expected gain cross-over frequency.

Normality and locality are the reason why the second-order LADRC and the PID control can be widely used. As shown in Example 1 and Example 2, double integrator (17) can be a local nominal model for a huge class of plants, including the plants with time-delay, unstable poles, and unstable zeros. with normality and locality, the second-order LADRC and the PID control are widely applicable for these plants.

Locality is a property to be proven. In Sects. 4 and 5, we prove the locality of the second-order LADRC and the PID control.

3.4 Operation stability

Operational stability is a concept Tsien proposes in Chapter 15 of [9]. It means the control system can stably work when the plant has large unpredictable variations. It implies perfect robustness and seems difficult.

Normality and locality can guarantee operational stability. With normality, the method may normalize two significantly different plants to the same local nominal model. With locality, the two plants obtain the same controller. If the two plants are respectively the plant before and after variation, operational stability is realized.

Example 3 Consider the plant (1)–(2) controlled by (5)–(8). Suppose at beginning, $(a_1, a_2) = (1, 0)$. Then at $t = 0.3s$, the plant suddenly changes and $(a_1, a_2) = (3.085, 100)$. It is a large variation because the plant loses its integrator. But with Fig. 2, we conclude the stability of the LADRC system is maintained, even the gain crossover frequency and phase margin vary little.

The time-domain simulation is shown in Figs. 5 and 6. The effect of the suddenly change on the state and control signals is indeed slight. That is, the system is operationally stable.

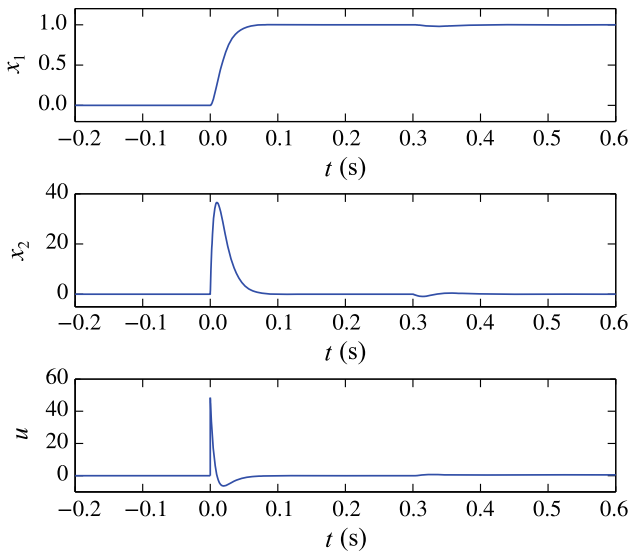

Fig. 5 The state and control signals of Example 3

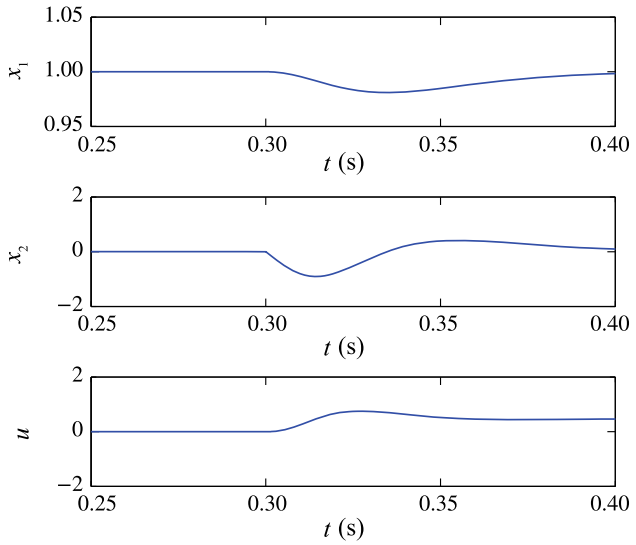

Fig. 6 The state and control signals of Example 3, around the variation moment $t = 0.3$

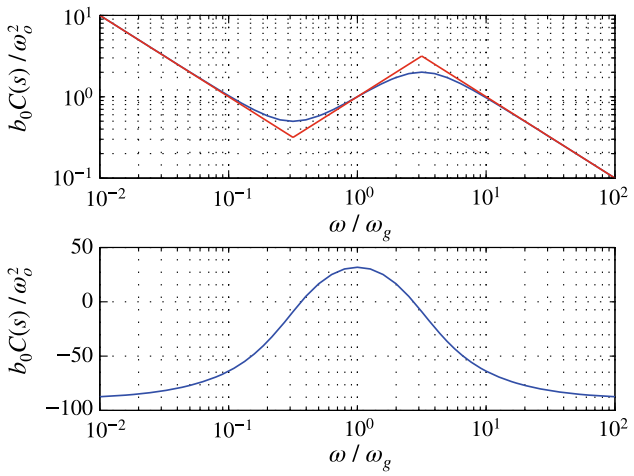

Fig. 7 Bode plot of $b_0C(s)/\omega_o^2$

4 Locally loop shaping

This section analyzes the locally loop-shaping ability of the second-order LADRC and the PID control, which is the foundation of the locality of the two approaches. Here locally loop shaping means to shape the loop transfer function's frequency response mainly with local information. We analyze the second-order LADRC first, then extend the results to the PID control.

4.1 Second-order LADRC

For the second-order LADRC (5)–(8), its controller (10) can be re-written as

$$C(s) = \frac{\omega_o^3(10s^2 + 5\omega_o s + \omega_o^2)}{b_0 s(s^2 + 5\omega_o s + 10\omega_o^2)} = \frac{\omega_o^2}{b_0} \cdot \frac{10\frac{s^2}{\omega_o^2} + 5\frac{s}{\omega_o} + 1}{\frac{s}{\omega_o}\left(\frac{s^2}{\omega_o^2} + 5\frac{s}{\omega_o} + 10\right)}.$$

It has two terms. The first term ω_o^2/b_0 is the gain, while the second term is a function of s/ω_o and can compensate phase.

The Bode plot of $b_0C(s)/\omega_o^2$ is drawn in Fig. 7, where the red line is the approximation of the magnitude plot. It has two break frequencies, $\omega_o/\sqrt{10}$ and $\sqrt{10}\omega_o$, which divide the Bode plot of $C(s)$ into three parts. The first is low frequency $\omega < \omega_o/\sqrt{10}$, where the magnitude descends with a slope approximating -1, while the phase approximates $-90°$. The second is middle frequency $\omega_o/\sqrt{10} < \omega < \sqrt{10}\omega_o$, where the magnitude increases with a slope approximating $+1$, while the phase increases then descends with a peak up to 31.9°. The third is high frequency $\omega > \sqrt{10}\omega_o$, where the magnitude descends with a slope approximating -1, while the phase approximates $-90°$.

Note that in low and high frequency, the phase of $C(s)$ is almost fixed. Only in middle frequency, the phase can be adjusted in a wide range. Or, only in middle frequency, by tuning ω_o and b_0, $C(s)$ can provide phase and gain compensation freely.

Because of its frequency response, $C(s)$ has a wonderful ability of locally loop shaping. Suppose $P(s)$ is the plant and consider the loop transfer function

$$L(s) = P(s)C(s).$$

With Fig. 7, we conclude that in low frequency $|L(\mathrm{j}\omega)|$ is enlarged, while large $|L(\mathrm{j}\omega)|$ is helpful to guarantee stability and reject the low-frequency external disturbance; In middle-frequency, the slope of $|L(\mathrm{j}\omega)|$ and $\angle L(\mathrm{j}\omega)$ are both adjusted to guarantee enough stability margin; In high frequency, $|L(\mathrm{j}\omega)|$ decreases quickly enough to be robust subject to unmodeled dynamics and filter measurement noise.

Furthermore, we have the following theorem.

Theorem 1 *If double integrator (17) is controlled by LADRC (5)–(8) with $b_0 = b$, then the system is stable. And the loop transfer function $P_0(s)C(s)$ has gain crossover frequency ω_o and phase margin* 31.9°, *while the magnitude plot has slope* -1 *at* ω_o.

Proof Let double integrator (17) be the plant in Fig. 1. The LADRC system's stability depends on the loop transfer function

$$P_0(s)C(s) = \frac{\omega_o^3(10s^2 + 5\omega_o s + \omega_o^2)}{s^3(s^2 + 5\omega_o s + 10\omega_o^2)}$$

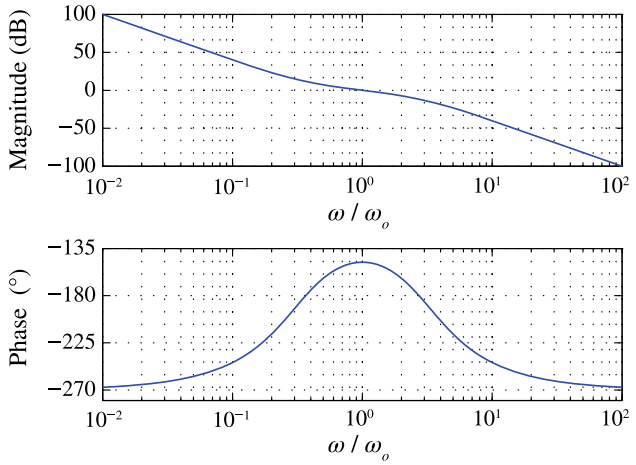

Fig. 8 Bode diagram of (23)

$$= \frac{10\left(\frac{s}{\omega_o}\right)^2 + 5\frac{s}{\omega_o} + 1}{(\frac{s}{\omega_o})^3\left[\left(\frac{s}{\omega_o}\right)^2 + 5\frac{s}{\omega_o} + 10\right]}, \tag{23}$$

which is a function of $\frac{s}{\omega_o}$ and has $|P_0(\mathrm{j}\omega_o)C(\mathrm{j}\omega_o)| = 1$. Furthermore,

$$\angle P_0(\mathrm{j}\omega_o)C(\mathrm{j}\omega_o)$$
$$= -180^\circ + \arctan\left(\frac{9}{5}\right) - \arctan\left(\frac{5}{9}\right) = -148.1^\circ.$$

Drawing the Bode diagram of $P_0(s)C(s)$ in Fig. 8, we conclude that the system is stable and $P_0(s)C(s)$ has unique gain crossover frequency. Thus, the gain crossover frequency is ω_o, while the phase margin is 31.9°. And it is easy to verify that the magnitude plot has slope -1 at ω_o. □

Theorem 1 and Fig. 8 establish a connection between double integrator (17) and LADRC (5)–(8). When $b_0 = b$, the controller (10) and the double integrator (17) make an ideal controller-plant pair. The transfer function $P_0(\mathrm{j}\omega_o)C(\mathrm{j}\omega_o)$ has an ideal shape. Especially, its gain crossover frequency is exactly the second tuning parameter ω_o, which can be arbitrarily tuned.

4.2 From second-order LADRC to PID control

Now we re-write (10) as

$$C(s) = \frac{\omega_o^2}{b_0} \cdot \frac{10\frac{s^2}{\omega_o^2} + 5\frac{s}{\omega_o} + 1}{\frac{s}{\omega_o}\left(\frac{s^2}{\omega_o^2} + 5\frac{s}{\omega_o} + 10\right)}$$
$$= \frac{\omega_o^2}{10b_0}\left(5 + \frac{1}{\frac{s}{\omega_o}} + 10\frac{s}{\omega_o}\right) \cdot \frac{10}{\frac{s^2}{\omega_o^2} + 5\frac{s}{\omega_o} + 10}.$$

Ignoring the term

$$\frac{10}{\frac{s^2}{\omega_o^2} + 5\frac{s}{\omega_o} + 10} \tag{24}$$

and defining

$$K_P = \frac{\omega_o^2}{2b_0}, \quad T_I = \frac{5}{\omega_o}, \quad T_D = \frac{2}{\omega_o},$$

$C(s)$ can be simplified as a PID controller

$$C_{\mathrm{PID}}(s) = \frac{\omega_o^2}{10b_0}\left(5 + \frac{\omega_o}{s} + 10\frac{s}{\omega_o}\right)$$
$$= K_P\left(1 + \frac{1}{T_I s} + T_D s\right). \tag{25}$$

Similarly, writing the pre-filter $C_1(s)$ as

$$C_1(s) = \frac{\omega_o^2}{10s^2 + 5\omega_o s + \omega_o^2} \cdot \frac{(s+\omega_o)^3}{\omega_o^3}.$$

and ignoring the term

$$\frac{(s+\omega_o)^3}{\omega_o^3}, \tag{26}$$

$C_1(s)$ can be simplified as

$$F_r(s) = \frac{\omega_o^2}{10s^2 + 5\omega_o s + \omega_o^2}. \tag{27}$$

Replacing $C(s)$ and $C_1(s)$ respectively with $C_{\mathrm{PID}}(s)$ and $F_r(s)$, we obtain the block diagram shown in Fig. 9.

Remark 7 If further ignoring the term $\frac{\omega_o^2}{10s^2+5\omega_o s+\omega_o^2}$ of $F_r(s)$, i. e., $F_r(s) = 1$, the PID control in Fig. 9 becomes a classical unity feedback PID control.

4.3 PID control

Note both (25) and (27) have two tuning parameters b_0 and ω_o, which are the two tuning parameters of the second-order LADRC. The Bode plots of $b_0C(s)/\omega_o^2$ and $b_0C_{\mathrm{PID}}(s)/\omega_o^2$

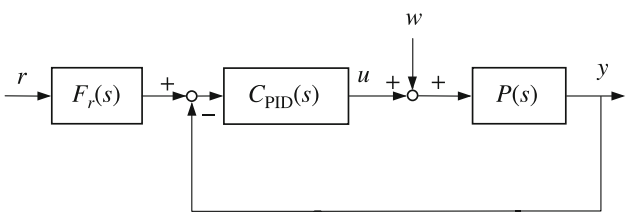

Fig. 9 Block diagram of the PID control

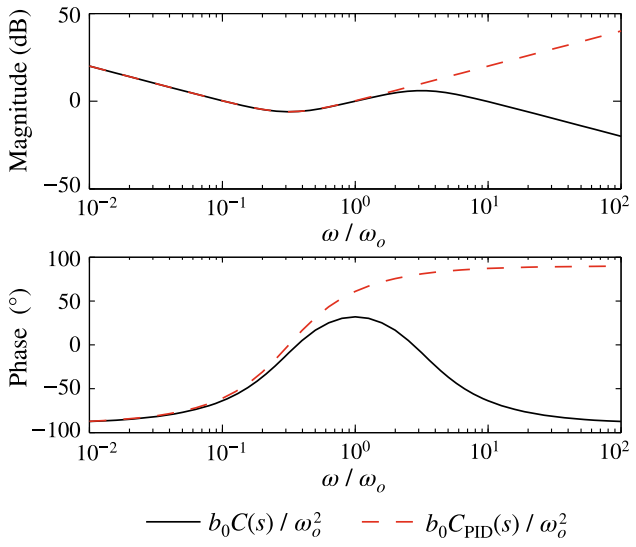

Fig. 10 Bode plots of $b_0C(s)/\omega_o^2$ and $b_0C_{\text{PID}}(s)/\omega_o^2$

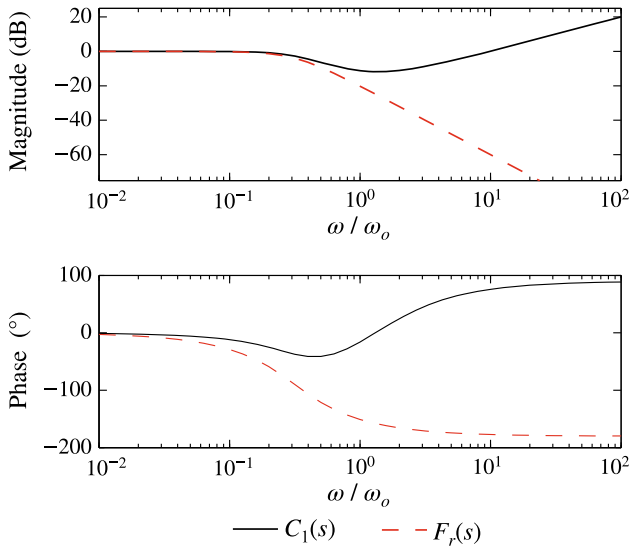

Fig. 11 Bode plots of $C_1(s)$ and $F_r(s)$

are draw in Fig. 10, while the Bode plots of $C_1(s)$ and $F_r(s)$ are drawn in Fig. 11. Since (24) and (26) have unity gain in low frequency, the two pairs are indeed close in low frequency. Note the phase plot of $b_0C_{\text{PID}}(s)/\omega_o^2$ illustrates the phase compensation is mainly in middle frequency around ω_o. In low and high frequency, $C_{\text{PID}}(s)$ has phase respectively approximating $-90°$ and $90°$.

Similar to the second-order LADRC, PID control has the following theorems.

Theorem 2 *Suppose double integrator (17) is controlled in Fig 9 as the plant. Then, with*

$$b_0 = \frac{\sqrt{106}}{10}b, \tag{28}$$

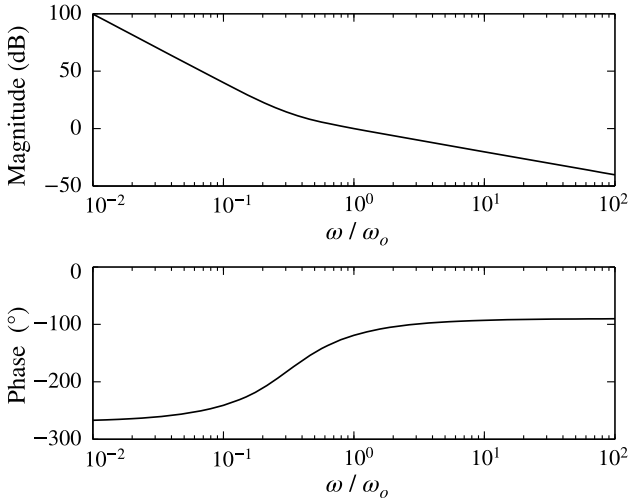

Fig. 12 Bode plot of $P_0(s)C_{\text{PID}}(s)$

the system is stable, while the loop transfer function $P_0(s)C_{\text{PID}}(s)$ has gain crossover frequency ω_o and phase margin 60.9°, and the magnitude plot's slope approximates -1 at ω_o.

Proof When (17) is controlled by $C_{\text{PID}}(s)$, the loop transfer function is

$$\begin{aligned} P_0(s)C_{\text{PID}}(s) &= \frac{b}{s^2}\cdot\frac{\omega_o^2}{10\frac{\sqrt{106}}{10}b}\left(5+\frac{\omega_o}{s}+10\frac{s}{\omega_o}\right) \\ &= \frac{\omega_o^2}{\sqrt{106}s^2}\left(5+\frac{\omega_o}{s}+10\frac{s}{\omega_o}\right). \end{aligned} \tag{29}$$

It is a function of $\frac{s}{\omega_o}$ and has $|P_0(\mathrm{j}\omega_o)C_{\text{PID}}(\mathrm{j}\omega_o)| = 1$, $\angle P_0(\mathrm{j}\omega_o)C_{\text{PID}}(\mathrm{j}\omega_o) = -119.1°$. Drawing the Bode diagram of $P_0(s)C_{\text{PID}}(s)$ in Fig. 12, we conclude that the system is stable and $P_0(s)C_{\text{PID}}(s)$ has unique gain crossover frequency. Thus, the gain crossover frequency is ω_o, while the phase margin is 60.9°. And it is easy to verify that the magnitude plot's slope approximates -1 at ω_o. □

5 The ADRC inspired design framework

In this section, we establish the locality of the second-order LADRC and the PID control. Then a design framework inspired by ADRC is proposed by generalization.

5.1 Locality as shown in second-order ADRC

Now we consider to control a plant $P(s)$ with the second-order LADRC. We assume

A1 the plant $P(s)$ has a local nominal model (17) at frequency $\omega_\gamma > 0$ and has no differentiator.

Theorem 3 *Suppose A1 holds. If $P(s)$ is controlled by LADRC (5)–(8) with*

$$b_0 = b, \quad \omega_o = \omega_\gamma, \tag{30}$$

then there exists $\omega_{\text{cut}} \approx \omega_\gamma$ such that

$$|P(\mathrm{j}\omega_{\text{cut}})C(\mathrm{j}\omega_{\text{cut}})| = 1, \tag{31}$$
$$\angle(P(\mathrm{j}\omega_{\text{cut}})C(\mathrm{j}\omega_{\text{cut}})) \approx -148.1^\circ. \tag{32}$$

Proof Consider the loop transfer function $P(s)C(s)$. Since $P(s)$ has no differentiator, it does not take place unstable pole-zero cancelation between $C(s)$ and $P(s)$. Because $P(s)$ has a local nominal model (17) at ω_γ, we conclude near ω_γ, $P(\mathrm{j}\omega)$ is continuous and has similar value and slope with $P_0(\mathrm{j}\omega)$. Then we have

$$P(\mathrm{j}\omega)C(\mathrm{j}\omega) \approx P_0(\mathrm{j}\omega)C(\mathrm{j}\omega), \quad \omega \approx \omega_\gamma. \tag{33}$$

Because of Theorem 1,

$$|P(\mathrm{j}\omega_\gamma)C(\mathrm{j}\omega_\gamma)| \approx 1, \tag{34}$$
$$\angle P(\mathrm{j}\omega_\gamma)C(\mathrm{j}\omega_\gamma) \approx -148.1^\circ, \tag{35}$$

and $|P(\mathrm{j}\omega_\gamma)C(\mathrm{j}\omega_\gamma)|$ has slope about -1. Thus, we conclude that $|P(\mathrm{j}\omega)C(\mathrm{j}\omega)|$ passes downstairs 0dB once near ω_γ. Let the passing frequency be ω_{cut}, we have (31) and (32). □

Theorem 3 establishes the locality of the second-order LADRC, which means the second-order LADRC (5)–(8) can be tuned based on local nominal model (17) and be used to control the plant $P(s)$. Suppose $P(s)$ is a typical engineering plant controlled by (5)–(8). The Bode plots of $P(s)C(s)$ and $P_0(s)C(s)$ are drawn in Fig. 13. Theorem 3 guarantees in the band near the expected gain crossover frequency ω_γ, $P(s)C(s)$ is close to $P_0(s)C(s)$. There exists ω_{cut} satisfying (31) and (32). Recalling Fig. 7, in low frequency we have $|P(\mathrm{j}\omega)C(\mathrm{j}\omega)| > 1$, while in high frequency we have $|P(\mathrm{j}\omega)C(\mathrm{j}\omega)| < 1$. Thus, $|P(\mathrm{j}\omega)C(\mathrm{j}\omega)|$ only passes 0dB once at ω_{cut}, the LADRC system is stable and has phase margin about 31.9°.

Theorem 3 should be used as a condition to try the second-order LADRC. When the plant satisfies A1, it is worth trying the second-order LADRC and has a great possibility to succeed.

Example 4 Consider the plant (18) in Example 2. Controlling it with LADRC (5)–(8), where $b_0 = 0.38$, $\omega_o = 1.7$, the Bode plots of $P(s)C(s)$ and $P_0(s)C(s)$ are what drawn in Fig. 13. It is easy to conclude that the LADRC stabilizes $P(s)$, although the Bode plots of $P(s)$ and $P_0(s)$ are quite different in low and high frequency.

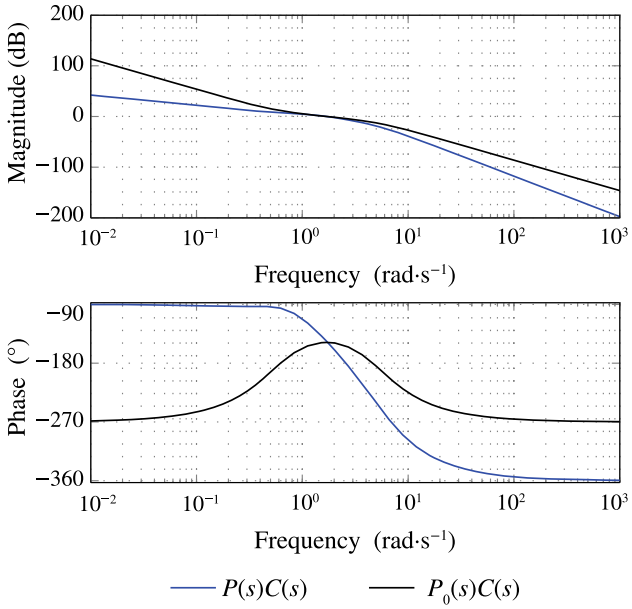

Fig. 13 Typical Bode plots of $P(s)C(s)$ and $P_0(s)C(s)$

Example 5 Re-consider the plant in Sect. 2.1. With Example 1 and Theorem 3, we conclude when (a_1, a_2) satisfying (14), the gain crossover frequency is near 100rad/s, while the phase margin is near 31.9°. For the pair of $(a_1, a_2) = (100, 0)$, the phase margin is significantly larger. That is what illustrated in Fig. 2.

Remark 8 Theorem 3 enlarges the scope to use the second-order LADRC. For example, the plants in Example 2 all can be controlled by the second-order LADRC.

Remark 9 With Theorem 3, ESO is an unnecessary high-gain in LADRC. High-gain means in ESO (5), the parameters $\beta_1, \beta_2, \beta_3$ are large enough. Or, when the three parameters are generated with (7), ω_o is large enough. In the existing ADRC literature, ESO is usually high-gain to guarantee the stability. But high-gain ESO is difficult to realize in practice. Theorem 3 proves that $\omega_o = \omega_\gamma$ is enough to guarantee stability, thus ESO is unnecessary high-gain.

5.2 Locality of PID control

Similar with Theorem 3, we have the following theorem, which establishes the locality for and is a trying condition of PID control.

Theorem 4 *Suppose the plant $P(s)$ satisfies A1 and is controlled in Fig 9 as the plant. Then, with*

$$b_0 = \frac{\sqrt{106}}{10}b, \quad \omega_o = \omega_\gamma, \tag{36}$$

then there exists $\omega_{\text{cut}} \approx \omega_\gamma$ *such that*

$$|P(\mathrm{j}\omega_{\text{cut}})C(\mathrm{j}\omega_{\text{cut}})| = 1, \tag{37}$$

$$\angle(P(\mathrm{j}\omega_{\text{cut}})C(\mathrm{j}\omega_{\text{cut}})) \approx -119.1^\circ. \tag{38}$$

Proof The proof is similar to the proof of Theorem 3. We consider the loop transfer function $P(s)C_{\text{PID}}(s)$. Since $P(s)$ has no differentiator, it does not take place unstable pole-zero cancelation between $C_{\text{PID}}(s)$ and $P(s)$. And we have

$$P(\mathrm{j}\omega)C_{\text{PID}}(\mathrm{j}\omega) \approx P_0(\mathrm{j}\omega)C_{\text{PID}}(\mathrm{j}\omega), \quad \omega \approx \omega_\gamma. \tag{39}$$

That is, in Bode diagram, the plot of $P(s)C_{\text{PID}}(s)$ is close to that of $P_0(s)C_{\text{PID}}(s)$. Thus,

$$|P(\mathrm{j}\omega_\gamma)C_{\text{PID}}(\mathrm{j}\omega_\gamma)| \approx 1, \tag{40}$$

$$\angle P(\mathrm{j}\omega_\gamma)C_{\text{PID}}(\mathrm{j}\omega_\gamma) \approx -119.1^\circ, \tag{41}$$

and $|P(\mathrm{j}\omega_\gamma)C_{\text{PID}}(\mathrm{j}\omega_\gamma)|$ has slope about -1. Because the Bode plot is continuous, we conclude that $|P(\mathrm{j}\omega)C_{\text{PID}}(\mathrm{j}\omega)|$ passes downstairs 0dB once near ω_γ. Let the passing frequency be ω_{cut}, we have (37) and (38). □

Example 6 Consider the plant in Example 1. Let $b = 206.25$, $\omega_\gamma = 100$, and generate PID control with (36). The Bode plots of $P(s)C_{\text{PID}}(s)$ for the five typical pairs are drawn in Fig. 14, while that of $P_0(s)C_{\text{PID}}(s)$ is also drawn. All five pairs are stable. For the four pairs of (14), the gain crossover frequency approximate ω_γ and phase margins are near 60.9°. While the pair $(a_1, a_2) = (100, 0)$ has a phase margin greater than 90°.

Remark 10 Theorem 4 clarifies when the differentiator (D) term is necessary. When the plant has the local nominal model (17) at the expected gain crossover frequency ω_γ, its phase approximates -180° there. In this situation, proportional-integral (PI) control can not obtain enough phase margin and D-term is necessary.

Remark 11 Theorem 4 implies the normality of PID control. With A1, PID control can be viewed as to normalize the plant to double integrator (17) first.

Remark 12 Theorem 4 can be used as a new tuning approach for PID control. It has only two tuning parameters and is similar with self-coupling PID in [24].

5.3 The design framework

The design framework is a generalization of the results of the second-order LADRC and the PID control. It obtains the controller in three steps.

Step 1 To establish a local nominal model (15) at the expected a gain crossover frequency ω_γ. In practice, such a ω_γ is usually given in the specification and by experienced engineers. Thus, complicated dynamics such as resonant peak are carefully avoid so that (15) can be a local nominal model and well describe the plant near ω_γ.

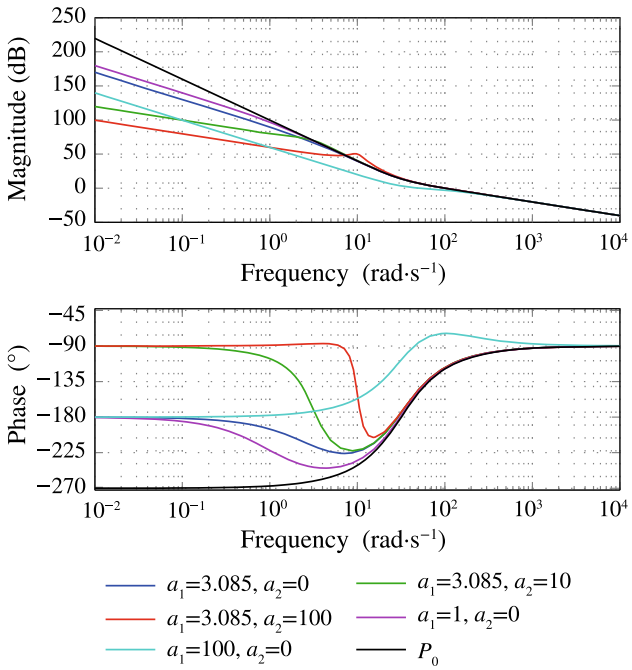

Fig. 14 Bode plots of $P(s)C_{\text{PID}}(s)$ and $P_0(s)C_{\text{PID}}(s)$ in Example 6

Step 2 To choose the corresponding controller based on local nominal model (15). For example, when $n = 1$ in (15), the first-order LADRC and the PI control are candidates; When $n = 2$, the second-order LADRC and the PID control are candidates; When $n = 3$, the third-order LADRC and the PIDD^2 control are candidates.

Step 3 To generate the controller's parameters. With these parameters, the controller provide gain and phase compensation at ω_γ exactly to local nominal model (15), and approximately to the plant. For LADRC, if $\omega_c = \omega_o = \omega_\gamma$ can not meet the phase margin specification, let $\alpha > 1$ be a tuning parameter and let

$$\omega_c = \frac{\omega_\gamma}{\alpha}, \quad \omega_o = \alpha\omega_\gamma, \tag{42}$$

then generate the parameters. For example, for the second-order LADRC, the parameters can be tuned with

$$\beta_1 = 3\omega_o, \quad \beta_2 = 3\omega_o^2, \quad \beta_3 = \omega_o^3,$$
$$l_1 = 2\omega_c, \quad l_2 = \omega_c^2.$$

By increasing α, the controller $C(s)$ can provide enough phase margin compensation at ω_γ. Then to tune b_0 to guarantee ω_γ is exactly the gain crossover frequency of the

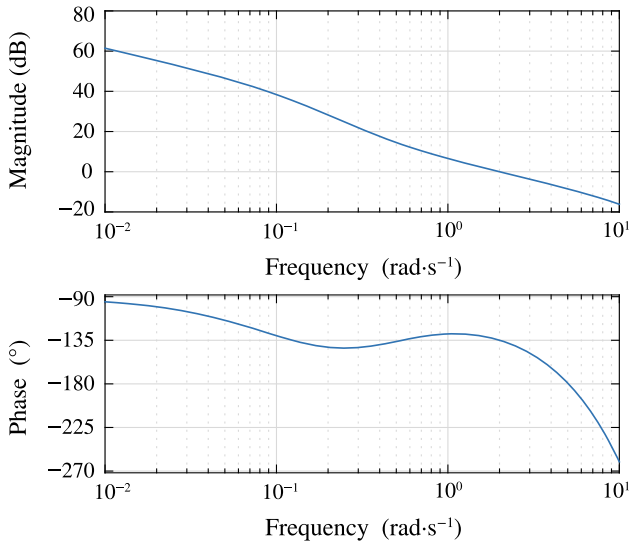

Fig. 15 Bode plots of $P_2(s)C(s)$ in Example 7

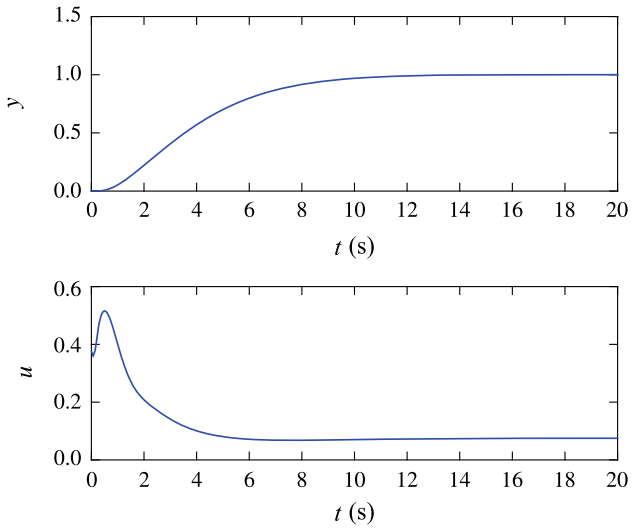

Fig. 16 Step response of Example 7

closed-loop. The details of tuning can be found in [25]. In this way, the controller can guarantee enough phase margin.

With the three steps, most plants can be controlled with enough phase margin, while to check stability and robustness is necessary in practice.

The following is an example to illustrate the design framework.

Example 7 Suppose to control the plant $P_2(s)$ in (19) with LADRC, the gain crossover frequency is specified as 2rad/s with phase margin 45°. Step 1, with Example 2, the local nominal model is (22). Step 2, the second-order LADRC is selected. Step 3, since 45° is obviously larger than 31.9°, we use $\alpha = 4$ in (42) and tune b_0 to 0.4479. The Bode diagram of $P_2(s)C(s)$ is drawn in Fig. 15. It indeed has gain crossover frequency 2rad/s and phase margin 45°. And the step response of the LADRC system is drawn in Fig. 16.

Remark 13 The controllers in Step 2 all have an integrator. If the integrator is not allowed because of the plant's differentiator or the type number specification, how to choose the candidate controllers is an open problem. Some preliminary work can be found in [26].

6 Conclusions

This paper showcases an ADRC-inspired design framework, combining insights from Tsien, Guan, and Han to justify and explain its inner workings. This framework rests on the notion of normality and locality as summarized below:

1. Normality. A large class of physical plants can be normalized in the form of an integrator chain, on which the controller is to be designed with ease and effectiveness. In ADRC design, once the order of the plant is determined, the plant is implicitly normalized as an integrator chain with the same order.

2. Locality. It is shown that the second-order LADRC and the PID control operate with locality. That is, these two approaches can obtain their controllers mainly with the local nominal model of the plant, while these controllers simultaneously compensate for the gain and phase freely only in the middle frequency, the neighborhood of the crossover.

3. A three-step design procedure is established: 1) establish the plant's local nominal model; 2) choose the corresponding controller, and 3) loop-shaping gain and phase in middle-frequency range. The second-order LADRC and the PID control are interpreted as two special examples in the new framework based on the same local nominal model of (17), leading to insight as to why the two control approaches have been used widely in practice.

4. Operational stability. Because the control design is not premised on the detailed and global model, the resulting closed-loop system proves to be robust in the presence of large variations in plant dynamics, as long as they do not alter the plant dynamics in the middle-frequency range. It is in this sense that the operational stability as defined by Tsien is attained.

References

1. Han, J. (1998). Auto-disturbance-rejection controller and its applications. *Control and Decision, 13*(1), 19–23. (in Chinese).
2. Han, J. (2008). *Active disturbance rejection control technique-the technique for estimating and compensating the uncertainties*. Beijing: National Defense Industry Press. (in Chinese).
3. Han, J. (2009). From PID to active disturbance rejection control. *IEEE Transactions on Industrial Electronics, 56*(3), 900–906.

4. Chen, Z., Liu, J., & Sun, M. (2018). Overview of a novel control method-active disturbance rejection control technology and its practical applications. *CAM Transactions on Intelligent Systems, 13*(6), 865–877.
5. Zheng, Q., & Gao, Z. (2018). Active disturbance rejection control: some recent experimental and industrial case studies. *Control Theory and Technology, 16*(4), 301–312.
6. Wu, Z., Gao, Z., Li, D., et al. (2021). On transitioning from PID to ADRC in thermal power plants. *Control Theory and Technology, 19*(1), 3–18.
7. Huang, Y., & Xue, W. (2014). Active disturbance rejection control: methodology and theoretical analysis. *ISA Transactions, 53*(4), 963–976.
8. Feng, H., & Guo, B.-Z. (2017). Active disturbance rejection control: old and new results. *Annual Reviews in Control, 44*, 238–248.
9. Tsien, H. S. (1954). *Engineering cybernetics*. NewYork, USA: McGraw-Hill.
10. Anderson, B. D. O. (2008). Arvin Dehghani, challenges of adaptive controlCpast, permanent and future. *Annual Reviews in Control, 32*(2), 123–135.
11. Guang, Z. (1980). Certain issues in modern control theory (I). *Acta Automatica Sinica, 6*(1), 49–56.
12. Han, J. (1989). Control theory: the doctrince of model or the doctrine of control? *Systems Science and Mathematical Sciences, 9*(4), 328–335. (in Chinese).
13. Zhou, R., Fu, C., & Tan, W. (2021). Implementation of linear controllers via active disturbance rejection control structure. *IEEE Transactions on Industrial Electronics, 68*(7), 6217–6226.
14. Tian, G., & Gao, Z. (2007). Frequency response analysis of active disturbance rejection based control system. In: *Proceedings of the 16th IEEE International Conference on Control Applications*, Singapore, IEEE, 1595-1599.
15. Xue, W., & Huang, Y. (2015). Performance analysis of active disturbance rejection tracking control for a class of uncertain LTI systems. *ISA Transactions, 58*, 133–154.
16. Zheng, Q., & Gao, Z. (2016). Active disturbance rejection control: between the formulation in time and the understanding in frequency. *Control Theory and Technology, 14*(3), 250–259.
17. Li, J., Xia, Y., Qi, X., et al. (2017). Robust absolute stability analysis for interval nonlinear active disturbance rejection based control system. *ISA Transactions, 69*, 122–130.
18. Liu, C., Luo, G., Chen, Z., et al. (2019). A linear ADRC-based robust high-dynamic double-loop servo system for aircraft electromechanical actuators. *Chinese Journal of Aeronautics, 32*(9), 2174–2187.
19. Jin, H., Song, J., Lan, W., et al. (2020). On the characteristics of ADRC: a PID interpretation. *Science China Information Science, 63*(10), 209201.
20. Herbst, G. (2021). Transfer function analysis and implementation of active disturbance rejection control. *Control Theory and Technology, 19*(1), 19–34.
21. Chen, S., Bai, W., Huang, Y., et al. (2020). On the conceptualization of total disturbance and its profound implications. *Science China Information Science, 63*, 129201.
22. Franklin, G. F., Powell, J. D., & Emami-Naeini, A. (2021). *Feedback control of dynamic systems* (8th ed.). Beijing: Publishing House of Electronics Industry.
23. Jin, H., & Lan, W. (2021). Second-order linear active disturbance rejection control for the double integrator: fast and nonovershooting step response. *Control Theory & Applications, 38*(9), 1486–1492. (in Chinese).
24. Zeng, Z., & Liu, W. (2021). Self-coupling PID controllers. *Acta Automatica Sinica, 42*(2), 404–422.
25. Jin, H., Song, J., Zeng, S., & et al. (2018). Linear active disturbance rejection control tuning approach guarantees stability margin. In: *Proceedings of the 15th International Conference on Control, Automation, Robotics and Vision (ICARCV)*, Singapore, IEEE, pp. 1132-1136
26. H. Jin, Y. Chen, W. Lan. (2019). Linear Active Disturbance Rejection Control With Partially Canceling Estimated Total Disturbance. In: *Proceedings of the 2019 IEEE International Conference on Real-time Computing and Robotics (RCAR)*, Irkutsk, Russia, IEEE, pp. 621-625

Huiyu Jin received his B. Eng., M. Eng., and Ph.D. degrees from University of Science and Technology of China in 1998, Shenyang Institute of Automation, Chinese Academy of Sciences in 2001, and University of Science and Technology of China in 2007 respectively. From 2001 to 2012 he was with University of Science and Technology of China. Since 2012 he has been with the Xiamen University where he is presently an assistant professor of School of Aerospace Engineering. He has been a visiting scholar with University of Southern California during 2010–2011 and with University of California, Irvine during 2016–2017. His research interests include active disturbance rejection control, data-driven control, nonlinear control, and their applications.

Zhiqiang Gao received his Ph.D. in Electrical Engineering from the University of Notre Dame in 1990 and has taught at Cleveland State University ever since. Faced with ever widening chasm between control theory and practice, Dr. Gao returned to the roots of controls by collaborating extensively with engineers at NASA and industry in solving real world problems, from which the foundation and authenticity of research were rebuilt. Collaborating with Prof. Jingqing Han, Dr. Gao worked quietly on active disturbance rejection control for over 20 years, nurturing it from its early, conceptual stage to a maturing and emerging industrial control technology. In doing so, he made an obscure idea clear and established firmly a general design principle in dealing with uncertainties in industrial settings, often with staggering improvements in performance and energy saving. Asking basic, rudimentary question in research and in teaching, Dr. Gao and his team find creative solutions in practice and vitality in education.